

## Thermal degradation and kinetic analysis of fly ash-enriched epoxy composites

M. Pandey<sup>1\*</sup>, P. Joshi<sup>2</sup>, S. Mehtab<sup>1</sup>, M. Aziz<sup>1</sup>, M. Pandey<sup>1</sup>, P. Kumar<sup>3</sup>, M.G.H. Zaidi<sup>1\*</sup>

<sup>1</sup>Department of Chemistry, College of Basic Sciences and Humanities, G.B. Pant University of Agriculture and Technology, Pantnagar, U.S Nagar-263145, Uttarakhand, India

<sup>2</sup>Department of Chemistry, School of Allied Sciences, Dev Bhoomi Uttarakhand University, Naugaon, 248007, India

<sup>3</sup>Department of Physics, Manipal University Jaipur, Jaipur-303007, Rajasthan, India

Received: May 17, 2023; Revised: June 20, 2023

Present investigation demonstrates the enrichment of fly ash (FA, 27.23 nm) into cured epoxy resin (CE) and the study of the non-isothermal kinetic mechanism and thermodynamic data of solid-state decomposition under oxidative media. Thermal study and degradation behavior of FA-enriched polymer composite (FEPc) were determined by simultaneous thermogravimetric (TG) - differential thermogravimetric (DTG) - differential thermal analysis (DTA). The kinetic parameters of FEPc were measured through Coats–Redfern (CR) and Horowitz–Metzger (HM) models under best-fit analysis and further evidenced by linear regression analysis. FEPc revealed two step decomposition with improved TG onset by 25 °C over CE due to the inherent thermal stability of FA. Results demonstrated that thermal behavior, kinetic and thermodynamic parameters of FEPc were improved with the enrichment of FA into CE. HM and CR models at reaction orders (n) ranging from 0 to 3 revealed the steadiness in order of solid-state degradation for CE (n = 2), FA and FEPc (n = 1) with negative value of entropy difference. CR method calculated higher values of activation energy ( $E_a$ ) over HM method. These applied methods delivered higher differences in the values of  $E_a$ , change in enthalpy and Gibbs free energy of solid-state degradations, but marginal changes in pre-exponential factor and change in entropy of FEPc over CE and FA. Kinetic and thermodynamic parameters disclosed modification in thermal stability of FEPc over CE due to the intrinsic thermal stability of FA.

**Keywords:** Fly ash, Cured epoxy, Polymer composite, Non-isothermal kinetics, Thermogravimetric analysis, Solid state degradation

### INTRODUCTION

Over past years, the kinetic analysis of non-isothermal decomposition procedures has been attracting the interest of many investigators along with modern history of thermal degradation. The kinetic analysis is necessary for correlating the kinetic and thermodynamic parameters to degradation mechanism [1, 2]. Thermal degradation mechanism allows the postulation of kinetic equations, and kinetics is the preliminary point to understand the mechanisms for decomposition [3]. Over other methods thermogravimetric analysis (TGA) is the most appropriate technique to study the kinetics [2, 4].

Epoxy resin (ER) is a thermosetting polymer which is characterized by at least one or more oxirane functional groups in the polymeric material and is regarded as reactive intermediate. ERs are primarily synthesized by the reaction of epichlorohydrin with active hydrogen of alcohols, phenols, acids, amines and through oxidation of olefins with peroxide [5, 6]. Di-glycidyl ether bisphenol-A (DGEBA) is a widely used bifunctional epoxy resin, synthesized by the reaction of epichlorohydrin with bisphenol A [7].

Furthermore, ERs can also react with active hydrogen of polyamines, polyphenols, polymercaptans and polyacids through polyaddition mechanism. Curing reaction of ER may be initiated in presence of UV light or appropriate catalysts at room or elevated temperatures through attack of a curing agent on the C-O-C ring. The curing reaction of ER is exothermic and mostly proceeds through step-growth polymerization [5, 7, 8]. High toughness, corrosion resistivity, moisture resistivity, mechanical and fatigue strength allows CE to be utilized in the field of protective coating, casting, automotive primer, glass sizing, electronic encapsulants, adhesives and aerospace composites [6, 9].

Various investigations have concluded to boost the thermal performance of ER through modification with electrical and thermally stable reinforcing agents [10]. Epoxy-based polymer composites (PCs) are of wide interest from an industrial and scientific viewpoint due to their exceptional characteristics over conventional composites [11]. Incessant demand of highly efficient materials encourages innovations in fabrication of PCs. Generally, PCs are incorporated with light-weight materials as fillers which attribute high mechanical and thermal

\* To whom all correspondence should be sent:  
E-mail: minakshipandey2912@gmail.com,  
mghzaidi@gmail.com

performance. These lightweight PCs are widely used in transportation, structural, automotive, aerospace, electronics, turbines and leisure industry [12-14]. The reinforcement of additives in ER have been under substantial attention over decades. Studies have shown that the thermal performance of epoxy composites has been improved by the reinforcement of various metallic [15], carbon-based materials [16, 17], hybrid [18], ceramic [19] and fly ash (FA) [2, 20] fillers.

Over the past decades FA has attracted interest due to its high abundance. It is made up of metallic oxides such as SiO<sub>2</sub>, Fe<sub>2</sub>O<sub>3</sub>, CaO and Al<sub>2</sub>O<sub>3</sub>. The presence of metallic oxides rises the thermo-mechanical performance of polymer composites [20]. FA is an industrial byproduct that results from the combustion of coal from thermal power plants, pulp, paper, brick making industries and incineration of municipal solid waste [21]. Composition of FA produced from different resources depends upon the type of coal, conditions of burning, combustion rate and cooling control. Global survey reveals production of about 780 MT / year of FA across the world out of which, 226.13 is nationally produced [22]. Globally, FA has been utilized in concrete and cement industries [23], synthesis of zeolites for wastewater treatment [24], geopolymer production [25], soil stabilization [26], and fabrication of polymer composites (PCs) [27, 28]. High bulk density, porosity, particle size and surface area allow FA usage as a suitable filler in the development of high-performance PCs [27]. Over the past years, FA has been used as reinforcement in epoxy-based polymers due to its enhanced electrical, mechanical thermal and electrochemical performance [28].

FA-enriched polymer composite (FEPc) has received emerging attention as naturally abundant, inexpensive and viable substitute for synthetic PCs applicable in thermal insulation of electrical and electronic devices [29]. Thermal insulation properties of PCs in construction industries play an important role for minimization the operational energy consumption. Thermal response of FEPc in the fire environment mainly depends on the thermal decomposition of FA. For this reason, Tiwari *et al.*, [2] developed different kinetic models for thermal degradation and curing kinetics tests on FA-reinforced PCs (2.5 to 7.5 wt%) to obtain the reaction kinetic parameters of the material and to explore decomposition mechanism. Thermal analysis of FA derived PCs reveals the kinetic and thermodynamic parameters, including pre-exponential factor, reaction order, change in entropy, enthalpy, Gibbs free energy and activation energy. Kinetic analysis reveals the higher value of

activation energy for Coats-Redfern (20.36 to 30.84) over Broido's (17.79 to 26.43) and Horowitz – Metzger (19.20 to 29.43) for first-order kinetics.

In the present investigation, FEPc was prepared and characterized through simultaneous TG-DTA-DTG. Kinetic and thermodynamic parameters such as activation energy ( $E_a$ ), frequency factor (A), enthalpy change ( $\Delta H$ ), entropy change ( $\Delta S$ ) and Gibbs free energy change ( $\Delta G$ ) associated with the materials were estimated from TGA through CR and HM methods.

### Materials

FA was collected from a thermal power plant, Kashipur, Uttarakhand, ground into 0.70 mm mesh size and dried at 40±1 °C. Commercially available DGEBA (ER, LY-556), with density 1.09 g/cm<sup>3</sup> and epoxy equivalent 197 g/Eq was used for development of FEPc. TETA (CY-230) and hexane (99.98%) were procured from Huntsman India Pvt Limited. Other chemicals and solvents (purity >99.55) were locally arranged and used without further purification.

### Preparation of FEPc

Stainless steel panels with 1 cm<sup>2</sup> area and 1.50±0.1 mm thickness were polished with emery paper followed by ultrasonic cleaning with acetone for 20 min. FEPc was developed through valorization of FA under enriched concentrations (60 phr) into epoxy resin. The process of development of FEPc involved dispersion of FA into ER in ethanol (2.0 mL) @ 500 rpm over 5 h to afford a suspension, followed by sequential thermal activation at 90±1°C over 1 h. The suspension was cooled to 40±1°C and cured with TETA hardener. This was followed by deposition of FEPc suspension on 316-SS current collectors. FEPc was kept at 25±1°C over 24 h thereafter post cured at 400 mm Hg/70°C.

### CHARACTERIZATION

Crystallite size (d) of FA was calculated through Debye Scherer equation  $D = K\lambda / \beta \cos\theta$ , where K=order of diffraction (K=1),  $\lambda$ =wavelength of X-ray,  $\beta$ =full width half maximum of peak,  $\theta$ =scattering angle [29]. Simultaneous TG-DTA-DTG was performed on EXSTAR TG/DTA 6300 in air @ 10 °C/min from ambient to 600°C with reference to alumina.

Kinetic models such as Horowitz–Metzger (HM) and Coats–Redfern (CR) were employed for calculation of the kinetic parameters including; order of reaction (n),  $E_a$ , A,  $\Delta S$ ,  $\Delta H$  and  $\Delta G$ . These methods depend on the conditions of experiments

and mathematical analysis of data fraction of thermal decomposition ( $\alpha$ ), was evaluated from TG data according to the relation:

$$\alpha = \frac{w_o - w_t}{w_o - w_f} = \frac{w_o - w_t}{w_o - w_f}$$

where,  $w_o$ = initial weight,  $w_t$ = weight at particular temperature and  $w_f$ = final weight of sample [30].

#### Coats-Redfern model

CR equation revealed the kinetic parameters in every stage of thermal degradation. CR method employs the plot of  $\log g(\alpha)$  against  $1000/T$  which

reveals the value of  $E_a$  through the slope  $(-\frac{E_a}{R})$  and pre-exponential factor (A) through the intercept  $\ln(\frac{ART^2}{\beta E_a}) \ln(\frac{ART^2}{\beta E_a})$ .

$$\log_{10} \left[ \frac{g(\alpha)}{T^2} \right] = \log_{10} \log_{10} \left[ \frac{AR}{\beta E} \left( 1 - \frac{2RT}{E_a} \right) \right] - \frac{E_a}{2.303RT}$$

For  $n = 0$ ,  $g(\alpha) = \alpha g(\alpha) = \alpha$ ;  $n = 1$ ,  $g(\alpha) = -\ln(1 - \alpha) g(\alpha) = -\ln(1 - \alpha)$ ;  $n = 2$

$$g(\alpha) = \frac{1}{1 - \alpha} g(\alpha) = \frac{1}{1 - \alpha}; \quad n=3$$

$$g(\alpha) = \frac{1}{(1 - \alpha)^2} g(\alpha) = \frac{1}{(1 - \alpha)^2} \text{ and for } n^{\text{th}} \text{ order}$$

$$g(\alpha) = [(1 - \alpha)^{1-n} - 1] / (n - 1)$$

$$g(\alpha) = [(1 - \alpha)^{1-n} - 1] / (n - 1)$$

where  $\beta$  = heating rate,  $R$  = gas constant (8.314 J/mol K) and  $T$  = degradation temperature.

The values of  $\Delta H$  (kJ/mol),  $\Delta S$  (kJ/mol.K) and  $\Delta G$  (kJ/mol) were calculated according to the

respective relation;  $E_a - RT, E_a - RT, R \ln \left( \frac{Ah}{kT} \right)$

$R \ln \left( \frac{Ah}{kT} \right)$  and  $\Delta H - T \Delta S, \Delta H - T \Delta S$ .

where  $k$  = Boltzmann constant ( $1.38 \times 10^{-23}$  J/K),  $h$  = Plank constant ( $6.626 \times 10^{-34}$  J.s) and  $R$  is universal gas constant (kJ/K. mol) [31].

#### Horowitz-Metzger model

HM equation illustrates the kinetic parameters of FA-reinforced PCs through the plot of  $\log_{10} \left[ \log_{10} \frac{w_o}{w_t} \right] \log_{10} \left[ \log_{10} \frac{w_o}{w_t} \right]$  over  $\theta$ , which reveals the value of activation energy through the

slope  $(-\frac{E_a}{2.303RT_s^2})(-\frac{E_a}{2.303RT_s^2})$  and pre-exponential factor (A) through the intercept

$$\log_{10} \left[ \frac{w_o - w_t}{w_o - w_f} \right] = \frac{E_a \theta}{2.303RT_s^2}$$

where,  $R$  is gas constant,  $w_o$  = initial weight of sample,  $w_t$  = weight of sample at a particular temperature and  $w_f$  = final weight of sample,  $T_s$  is reference temperature and is appraised as the temperature at which  $w_t/w_o = 0.37$  for  $n = 1$  of the degradation process,  $\theta$  is the difference between

the peak temperature and the temperature at a particular weight loss ( $\theta = T - T_s$ ) [30]. The values of  $\Delta H$ ,  $\Delta S$  and  $\Delta G$  were calculated according to the above-mentioned relation.

## RESULTS AND DISCUSSION

### Thermogravimetric analysis

Thermal stabilities of FA CE and a respective FEPc were examined through simultaneous TG-DTA-DTG from ambient conditions to 600°C. TG reveals the weight loss (%wt) with respect to temperature @ 10°C/min in air. DTG demonstrates the maximum rate of degradation ( $\mu\text{g}/^\circ\text{C}$ ) at the respective peak decomposition temperature. However, DTA reveals the fusion temperature at the respective peak temperatures ( $^\circ\text{C}$ ).

TG of FA revealed single step rapid decomposition up to 600°C leaving a weight residue (Wr) of 96.7 % and was associated with 0.8% moisture content. This was supported by DTG @ 5.8 ( $\mu\text{g}/^\circ\text{C}$ ) at 212°C. Not any single peak was observed in DTA analysis which attributes to amorphous nature of FA.

TG of CE revealed three-step decomposition - first step decomposition with TGo at 185°C leaving 87.5% Wr due to degradation of residual monomers of CE and untreated reagents. Such decomposition of CE was supported with a DTG signal @ 27.5  $\mu\text{g}/^\circ\text{C}$  at 219  $^\circ\text{C}$ . Prior to this temperature, CE was decomposed leaving 98.3 % Wr at 163°C due to loss of moisture content (0.40 %) and untreated reagents. Second step decomposition of CE revealed TGo at 300  $^\circ\text{C}$  leaving 74.2% Wr. Within the range of temperature 300–363  $^\circ\text{C}$ , the maximum weight loss (38%) was due to breakage of ether bond and C-C bond of benzene ring. Major decomposition of CE was supported with DTG signal @ 88.0  $\mu\text{g}/^\circ\text{C}$  at 350  $^\circ\text{C}$ . CE has revealed a DTA signal of 49.2  $\mu\text{V}$  at 360  $^\circ\text{C}$  with heat of fusion -136.3 J/g. Third step decomposition of CE showed TGo at 363  $^\circ\text{C}$  leaving 36.2% Wr. This decomposition was further supported with a DTG signal @ 37.5  $\mu\text{g}/^\circ\text{C}$  at 418°C. TGe of CE appeared at 458  $^\circ\text{C}$  leaving 7.5 % char residue.

Thermal degradation of FEPc showed two-step decomposition. FEPc revealed first step decomposition with TGo at 210°C leaving 94.7 % Wr. Such decomposition progressed with @ 6.9  $\mu\text{g}/^\circ\text{C}$  at 183°C. Prior to this temperature, weight loss of 5.3% attributed to expulsion of moisture content (1.8%) and untreated residual monomer of CE. Second step decomposition of FEPc was initiated with TGo at 301  $^\circ\text{C}$  leaving 91.9 %Wr. Such decomposition was further supported with DTG

signal @ 54.0  $\mu\text{g}/^\circ\text{C}$  at 370 $^\circ\text{C}$ . TGe of FEPC appeared at 500  $^\circ\text{C}$  leaving 55.1 % char residue.

**Table. 1.** Thermal parameters of FA, CE and respective FEPC.

	$[\text{TG}_0(\text{TG}_e)]^A$	$\text{DTG}^B$
CE	162 (98.3) 500 (7.5)	27.5 (219), 88.0 (350), 418 (37.5)
FA	200 (98.8) 600 (97.7)	5.9 (220) 3.5 (500)
FEPC	200 (94.7) 500 (55.1)	54.0 (370)

A:  $\text{TG}_0 = \% \text{Wr}$  at TG onset ( $^\circ\text{C}$ ),  $\text{TG}_e = \% \text{Wr}$  at TG endset ( $^\circ\text{C}$ ). B: Rate of degradation,  $\mu\text{g}/^\circ\text{C}$  (Peak temperature,  $^\circ\text{C}$ ).

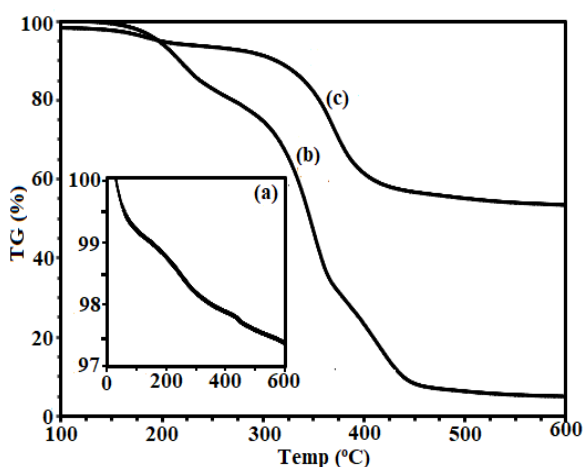


**Fig. 1.** TG of FA(a), CE(b) and FEPC(c)

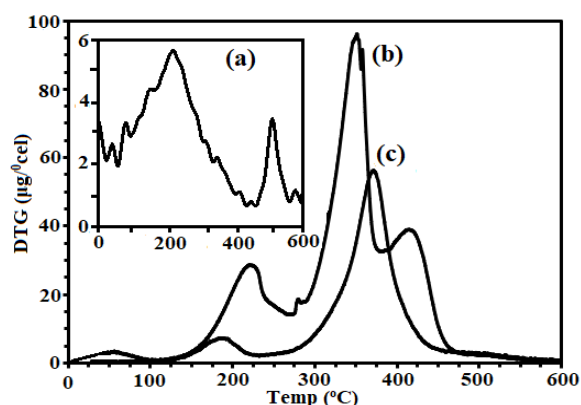


**Fig. 2.** DTG of FA(a), CE(b) and FEPC (c)

### Kinetic analysis

Kinetic analysis of FA, CE and FEPC through non-isothermal decomposition methods revealed  $E_a$ ,  $A$ ,  $\Delta S$ ,  $\Delta H$  and  $\Delta G$ . Respective thermodynamic and kinetic parameters were deduced from TGA analysis using HM and CR for  $n = 0, 1, 2, 3$  and are also summarized in Table 2. Regression coefficients ( $R^2$ ) ( $n = 0$  to 3) of order.

evaluated from CR and HM plots attributed their satisfactory linear relation (Table 2).

In general, the respective  $A$  and  $E_a$  of FA, CE and FEPC evaluated from CR method have higher value over HM method in the entire range .

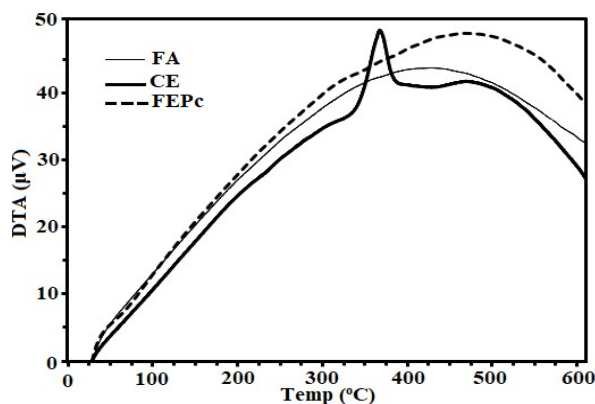


**Fig. 3.** DTA of FA(a), CE(b) and FEPC(c)

Generally, CR method reveals higher  $E_a$  over HM method [2]. CR and HM methods have disclosed larger variation in the values of  $E_a$ ,  $\Delta G$  and  $\Delta H$  but only a slight difference in the values of  $\Delta S$ . In general, FA, CE and FEPC, their respective  $E_a$  and  $A$  evaluated from CR method were higher over HM method. However, an insignificant difference was observed in the values of  $\Delta S$  evaluated from HM and CR methods.

FA revealed that  $E_a$  ranges between 45.16 and 26.87 (50.30 to 35.39). For CE and related FEPC, CR (HM) methods disclosed  $E_a$  ranging from 11.43 to 14.56 (15.23 to 24.25) and 33.01 to 53.31 (42.74 to 40.23), respectively. Exceptionally higher values of  $E_a$  for FA and related FEPC, revealed enhanced thermal stability. For FA, CR the HM method revealed  $A$  ranging from 0.34 to 5.66 (0.23 to 4.32). For CE and respective FEPC, CR the HM method revealed  $A$  ranging from 1.23 to 1.31 (1.25 to 1.32) and 2.94 to 2.71 (2.68 to 2.89), respectively.

For FA, CR the HM method revealed ( $-\Delta S$ ) ranging from 0.12 to 0.22 (0.15 to 0.24). CE and related FEPC attributed ( $-\Delta S$ ) ranging from 0.25 to 0.28 (0.24 to 0.29) and 0.25 to 0.12 (0.32–0.15) respectively. For FA, CR the HM method attributed ( $\Delta H$ ) ranging from 39.98 to 21.69 (45.13 to 30.11). For CE and related FEPC, CR the HM method attributed ( $-\Delta H$ ) ranging from 6.00 to 9.21 (10.05 to 19.07) and 27.82 to 48.13 (37.56 to 35.06) respectively. For FA, CR the HM method attributed ( $\Delta G$ ) ranging from 114.74 to 158.75 (138.58 to 179.63). For CE and related FEPC, CR the HM method attributed ( $\Delta G$ ) ranging from 166.75 to 182.80 (159.57 to 199.74) and 183.57 to 122.89 (217.60 to 131.51), respectively.

**Table 2.** Kinetic and thermodynamic parameters of FA, CE and respective FEPc evaluated from CR and HM models.

	T (K)	n	Method	Ea <sup>a</sup>	A <sup>b</sup>	-ΔS <sup>c</sup>	ΔH <sup>a</sup>	ΔG <sup>a</sup>	R <sup>2</sup>
FA	623	0	HM	45.16	0.34	0.12	39.98	114.74	0.9951
			CR	50.30	0.23	0.15	45.13	138.58	0.9952
		1	HM	25.36	0.25	0.25	20.18	175.93	0.9982
			CR	30.24	0.24	0.23	25.06	168.35	0.9987
		2	HM	50.90	1.79	0.32	45.72	245.08	0.9972
			CR	52.32	0.26	0.35	47.14	265.19	0.9965
3	HM	26.87	5.66	0.22	21.69	158.75	0.9921		
	CR	35.29	4.32	0.24	30.11	179.63	0.9952		
CE	623	0	HM	11.35	1.23	0.25	6.00	166.75	0.9953
			CR	15.23	1.25	0.24	10.05	159.57	0.9952
		1	HM	17.53	0.98	0.27	12.18	185.79	0.9923
			CR	23.89	1.00	0.29	18.71	199.38	0.9914
		2	HM	19.28	0.85	0.19	13.93	136.10	0.9989
			CR	20.36	1.25	0.21	15.18	146.01	0.9982
3	HM	14.56	1.31	0.28	9.21	182.80	0.9912		
	CR	24.25	1.32	0.29	19.07	199.74	0.9920		
FEPc	643	0	HM	33.01	2.94	0.25	27.82	183.57	0.9893
			CR	42.74	2.68	0.28	37.56	217.60	0.9912
		1	HM	43.74	5.54	0.23	38.56	181.85	0.9993
			CR	52.36	5.23	0.25	47.18	207.93	0.9985
		2	HM	36.09	7.75	0.31	30.91	224.04	0.9975
			CR	36.95	5.63	0.32	31.77	237.53	0.9982
3	HM	53.31	2.71	0.12	48.13	122.89	0.9912		
	CR	40.23	2.89	0.15	35.06	131.51	0.9923		

<sup>a</sup>: KJmol<sup>-1</sup>; <sup>b</sup>: min<sup>-1</sup>; <sup>c</sup>: KJmol<sup>-1</sup> K<sup>-1</sup>

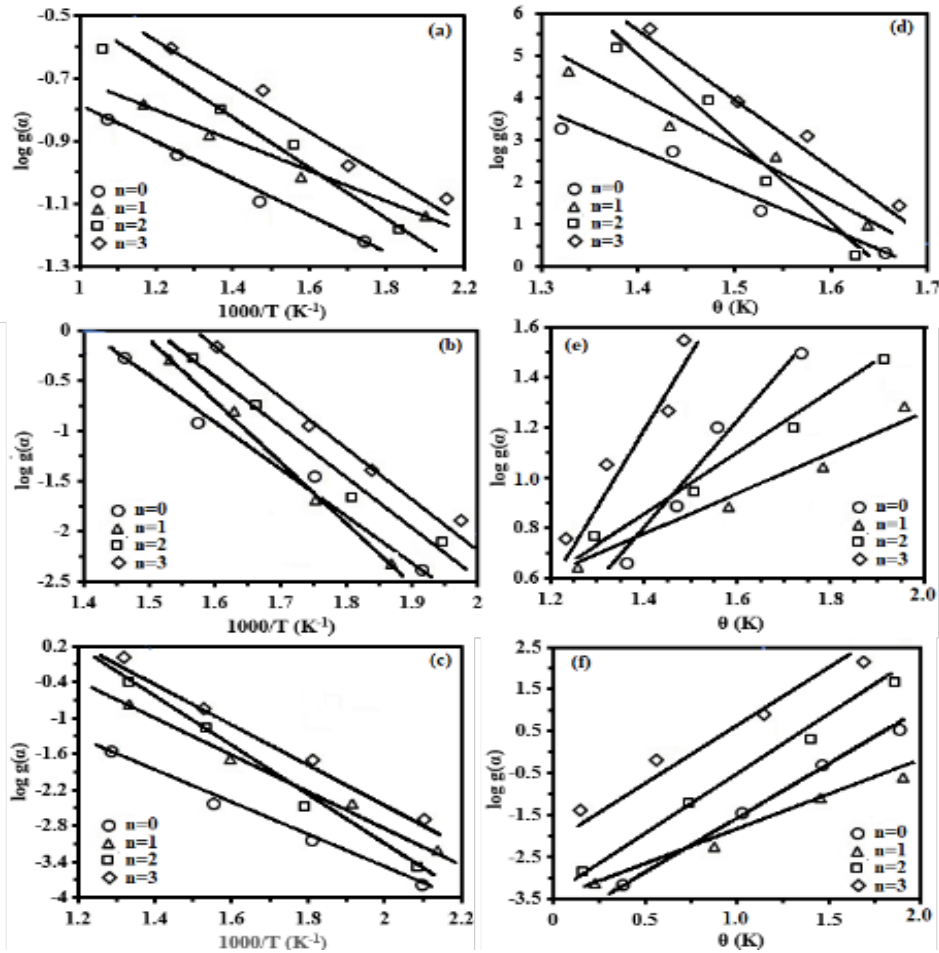


**Fig. 4.** CR thermogram of FA (a), CE (b), FEPc (c) and HM thermogram of FA (d), CE (e) and FEPc (f).

## CONCLUSION

Fly ash-enriched polymer composite (FEPc) was prepared through curing reaction of fly ash (FA, 60 wt%) with an epoxy based reactive binder. For this investigation, FA (0.80% moisture content) was procured from nearby thermal plant. Non-isothermal kinetic, thermal and thermodynamic data of FEPc were compared with FA and CE. Thermogravimetric analysis @10°C heating rate was employed to evaluate the kinetic and thermodynamic parameters of the materials through Coats–Redfern (CR) and Horowitz–Metzger (HM) models at  $n = 0, 1, 2$  & 3. The activation energy, pre-exponential factor and order of reaction of FEPc were improved due to the enrichment of FA into cured epoxy (CE). CR model attributed greater value of activation energy ( $E_a$ ) and frequency factor (A) over HM model for all materials. Non-isothermal kinetic parameters were obtained through plotting calculated values of  $\log(\alpha)$  against decomposition temperature.  $E_a$  and A values of the materials attributed that CE follows second order kinetics while FA and FEPc follow first order kinetics. The obtained results concluded that FA is the most impressive reinforcing agent for improving the thermal stability of the CE, which leads to shifting of weight loss stages to higher decomposition temperatures along with an increment in the char residue @ 600°C. Higher thermal stability of FEPc makes them suitable to use in anticorrosive coatings, electrical and microelectronic devices.

**Acknowledgement:** Financial support from Defence Research and Development Organization Research Grant No. ERIP/ER/0703649/M/01/1092 funded for the research facilities by the Government of India acknowledged. Senior research fellowship granted to Minakshi Pandey vide grant No.09/171/(0134)2019-EMI-I from the Council of Scientific and Industrial Research & University Grants Commission India are also hereby acknowledged.

## REFERENCES

1. J. B. Dahiya, K. Kumar, M. Muller-Hagedorn, H. Bockhorn, *Polym. Int.*, **57**, 722 (2008).
2. S. Tiwari, C. L. Gehlot, K. Srivastava, D. Srivastava, *J. Ind. Chem. Soc.*, **98** (5) 100077 (2021).
3. G. Léonard, D. Toye, G. Heyen, *Int. J. Greenh. Gas Control.*, **30**(6), 171 (2014).
4. R. Ebrahimi-Kahrizsangi, M. H. Abbasi, *Trans. Nonferrous Met. Soc. China*, **18** (1), 217 (2008).
5. C. Chen, B. Li, M. Kanari, D. Lu, *Adhes. Adhes. Joints Ind. Applications*, **37** (2019).
6. Z. Yan, J. Tian, K. Wang, K. D. Nigam, G. Luo, *Chemical Engineering Science*, **229**, 116071 (2021).
7. W. Zhou, D. Lv, H. Ding, P. Xu, C. Zhang, Y. Ren,

- .... P. Ma, *React. Funct. Polym.*, **180**, 105383 (2022).
8. C. Liu, M. Sun, B. Zhang, X. Zhang, G. Xue, X. Zhang, *Eur Polym. J.*, **121**, 109304 (2019).
9. A. C. Marques, A. Mocanu, N. Z. Tomić, S. Balos, E. Stammen, A. Lundevall, ... S. Teixeira de Freitas, *Materials*, **13** (24), 5590 (2020).
10. Z. R. Jia, Z. G. Gao, D. Lan, Y. H. Cheng, G. L. Wu, H. J. Wu, *Chin. J. Phys. B.*, **27** (11), 117806 (2018).
11. M. Hemath, S. Mavinkere Rangappa, V. Kushvaha, H. N. Dhakal, S. Siengchin, *Polym. Compos.*, **41** (10), 3940 (2020).
12. G. Roviello, L. Ricciotti, O. Tarallo, C. Ferone, F. Colangelo, V. Roviello, R. Cioffi, *Materials*, **9** (6), 461 (2016).
13. A. Pattanaik, M. Mukherjee, S. B. Mishra, *Compos. B: Eng.*, **176**, 107301 (2019).
14. R. Manimaran, I. Jayakumar, R. Mohammad Giyahudeen, L. Narayanan, *Energ. Source. Part A: Recovery, Utilization. Env. Effects*, **40** (8), 887 (2018).
15. A. I. Misiura, Y. P. Mamunya, M. P. Kulish, *J. Macromol. Sci. Part B.*, **59** (2), 1216 (2020).
16. I. Bustero, I. Gaztelumendi, I. Obieta, M. A. Mendizabal, A. Zurutuza, A. Ortega, B. Alonso, *Adv. Compos. Hybrid Mater.*, **3**, 31 (2020).
17. E. C. Senis, I. O. Golosnoy, J. M. Dulieu-Barton, O. T. Thomsen, *J. Mater. Sci.*, **54** (12), 8955 (2019).
18. M. W. Akhtar, J. S. Kim, M. A. Memon, M. M. Baloch, *Compos. Sci. Technol.*, **195**, 108183 (2020).
19. Y. Ouyang, L. Bai, H. Tian, X. Li, F. Yuan, *Compos. Part A: Appl. Sci. Manuf.*, **152**, 106685 (2022).
20. S. Tiwari, K. Srivastava, C. L. Gehlot, D. Srivastava, *Int. J. Waste Resour.*, **10**, 1 (2020).
21. S. S. Alterary, N. H. Marei, J. King Saud Univ. Sci., **33** (6), 101536 2021.
22. S. K. John, Y. Nadir, K. Girija, *Constr. Build Mater.*, **280**, 122443 (2021).
23. S. Pangdaeng, T. Phoongernkham, V. Sata, P. Chindaprasirt, *Mater. Des.*, **53**, 269 (2014).
24. C. L. Hwang, C. H. Chiang, T. P. Huynh, D. H. Vo, B. J. Jhang, S. H. Ngo, *Constr. Build Mater.*, **135**, 459 (2017).
25. Z. Zhang, H. Wang, Y. Zhu, A. Reid, J. L. Provis, F. Bullen, *Appl. Clay Sci.*, **88**, 194 (2014).
26. Z. Luo, B. Luo, Y. Zhao, X. Li, Y. Su, H. Huang, Q. Wang, *Polymer*, **14** (2), 307 (2022).
27. J. Sim, Y. Kang, B. J. Kim, Y. H. Park, Y. C. Lee, *Polymer.*, **12** (1), 79 (2020).
28. M. Gnanavel, T. Maridurai, K. M. Kumar, *Mater. Res. Express.*, **6** (9), 095507 (2019).
29. M. Pandey, S. Mehtab, M. G. H. Zaidi, *Mater. Today: Proc.*, **65**, 3278 (2022).
30. P. Joshi, G. Bisht, S. Mehtab, M. G. H. Zaidi, *Mater. Today: Proc.*, **62**, 6814 (2022).
31. H. Li, N. Wang, X. Han, H. Yuan, J. Xie, *Polymer*, **13** (4), 569 (2021).